Candida albicans induce hypoxia response via activating EGFR to promote colorectal cancer progression

Wanqiu Wang[1,*], Haihuang Li[1], FangLei Gong[1], Zhenyu Zhang[1], Yanping Ma[2], Yu Zhao[3], Changzheng Du[4,5], Ningning Li[6], Guiwei He[2,*], Kun Sun[1,*]

[1]Institute of Cancer Research, Shenzhen Bay Laboratory, Shenzhen 518132, China

[2]Institute of Infectious Diseases, Shenzhen Bay Laboratory, Shenzhen 518132, China

[3]Molecular Cancer Research Center, School of Medicine, Shenzhen Campus of Sun Yat-sen University, Sun Yat-sen University, Shenzhen 518107, China

[4]Beijing Tsinghua Changgung Hospital, Tsinghua University School of Medicine, Beijing 102218, China

[5]Department of Biochemistry, School of Medicine, Southern University of Science and Technology, Shenzhen 518055, China

[6]Tomas Lindahl Nobel Laureate Laboratory, The Seventh Affiliated Hospital, Sun Yat-Sen University, Shenzhen 518107, China

[*]Corresponding authors: wangwq@szbl.ac.cn (W.W.), hegw@szbl.ac.cn (G.H.), and sunkun@szbl.ac.cn (K.S.).

Keywords: microbiome, tumor microenvironment, candidalysin, NF-kappaB, fungi

Abstract

Colorectal cancer (CRC) is one of the leading causes of cancer-related mortality worldwide. Gut microbiota, including fungi, are considered to associate with CRC progression, while their functions and underlying mechanisms remain largely elusive. Here, we assessed the engagement of *Candida albicans* (*C. albicans*), a common fungus, in CRC progression. Using a cell-fungi co-culture system, we found that *C. albicans* could activate critical pro-metastatic genes and pathways, including MAPK and NF-κB, to up-regulate the expression of transcription factor, c-Jun, and c-Myc. Subsequently, c-Jun and c-Myc provoked hypoxia inducible factor 1α (HIF-1α) stabilization at normoxia, which further promote angiogenesis and tumor progression. Loss-of-function investigation showed that during this procedure, the virulence factor candidalysin secreted by *C. albicans* was essential for eliciting cancer cell responses through inducing the phosphorylation of epidermal growth factor receptor (EGFR) and Toll-like Receptors (TLRs) in the tumor cell, preferably in a species and cancer cell-dependent manner. The activation of hypoxia pathway by *C. albicans* was reinforced in colon organoids derived from CRC specimens. Hence, our results demonstrated that *C. albicans* activated the EGFR/TLR2 - ERK/NF-κB - HIF-1α signaling pathway and induced a hypoxia response to promote cancer progression, thereby presenting a potential therapeutic target for CRC treatment.

Introduction

Colorectal cancer (CRC) is one of the leading causes of cancer-related mortality worldwide[1]. The majority of CRC deaths are attributed to disease progression and metastasis[2], therefore, understanding the intricate mechanisms underlying CRC progression is imperative for improving patient outcomes. Numerous factors have been proposed to be involved in CRC metastasis, including the gut microbiota, a diverse community of microorganisms (including bacteria, viruses, and fungi) closely linked to human health and cancer[3–8]. In particular, dysbiosis of the fungal microbiota is implicated in various cancer types[9–14]. For instance, the absence of receptor proteins responsible for recognizing fungi has been linked to the promotion of colorectal tumorigenesis[15,16]. Among the known fungi, *Candida albicans* (*C. albicans*), an opportunistic pathogenic fungus commonly found in the human intestinal tract, can proliferate under conditions of immunosuppression or microbiome dysbiosis and leads to candidiasis[17]. Once adhering to host cells via adhesins, *C. albicans* transitions from its yeast form to a hyphal form, enabling it to penetrate host tissues and invade epithelial barriers[18–20]. Moreover, *C. albicans* secretes virulence factors, such as candidalysin, which can directly damage host cells and activate host immune responses[21]. In CRC, *C. albicans* is more frequently detected in tumors compared to non-cancerous tissues, indicating a potential role in tumorigenesis and progression[22]. Recent studies have uncovered important interplay between *C. albicans* and the tumor microenvironment[23,24,25]. In particular, Zhu and colleagues showed that in mouse models, *C. albicans* colonization induces higher tumor load and more severe colitis[25]. However, involvement of *C. albicans* in CRC progression and the molecular mechanism are still largely elusive.

In this study, using a co-culture system, we investigated the influence of *C. albicans* infection on CRC as well as the molecular-level changes triggered by *C. albicans* to explore the mechanism

underlying its role in CRC development and progression.

Results

C. albicans is associated with CRC progression

Given that *C. albicans* is a predominant gut fungus implicated in CRC, we first investigated its presence and abundance in colorectal adenocarcinoma samples from The Cancer Genome Atlas (TCGA) project[26]. As shown in Fig. 1b-c, the abundance of *C. albicans* is significantly increased in late-stage CRC patients and correlates with poorer prognosis. To validate this result, we recruited four colorectal cancer patients (two in stage II and two in stage III) and collected the tumor samples post-surgery. Interestingly, we found that fungi were present in both stage III patients, while not in stage II patients (Figure 1a). Moreover, we observed the presence of fungi surrounding tumor cells (Figure 1d). To elucidates the influence of *C. albicans* on CRC, we co-cultured the CRC cell line HCT116 with *C. albicans.* Our results showed that *C. albicans* significantly enhanced cell migration. This effect persisted even in the presence of colon bacterium *Bacteroides fragilis*, which is known to suppress the growth of *C. albicans* (Figure 1e-f). We then examined epithelial-mesenchymal transition (EMT), a crucial process in cancer progression and metastasis. Analysis of EMT marker gene expression confirmed that *C. albicans* infection reduced E-cadherin levels while increasing Vimentin and Slug expression (Figure 1g, Suppl. Figure S1a). Immunofluorescence staining revealed a reduction in E-cadherin at infection sites, with co-localization of E-cadherin signals and the C. albicans cell wall, suggesting a direct interaction between C. albicans and the HCT116 cell membrane (Figure 1h, Suppl. Figure S1b). Collectively, these findings suggest that *C. albicans* contributes to late-stage CRC progression by promoting cell migration and EMT.

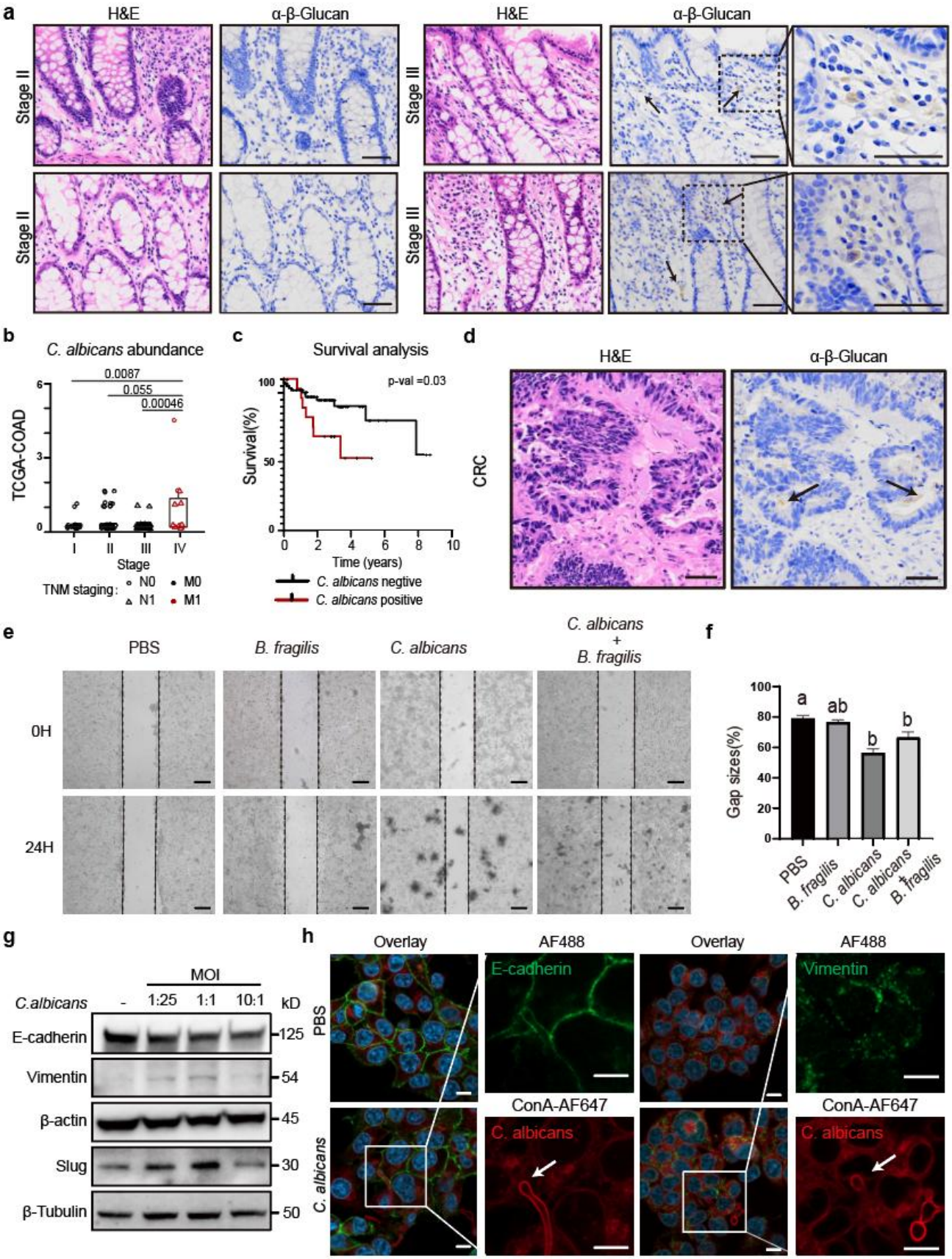
a
H&E
α-β-Glucan
Stage II
Stage III
b
C. albicans abundance
TCGA-COAD
0.0087
0.055
0.00046
Stage
TNM staging:
N0
N1
M0
M1
c
Survival analysis
p-val =0.03
Survival(%)
Time (years)
C. albicans negtive
C. albicans positive
d
CRC
e
PBS
B. fragilis
C. albicans
C. albicans + B. fragilis
0H
24H
f
Gap sizes(%)
PBS
B. fragilis
C. albicans
C. albicans + B. fragilis
g
C.albicans
MOI
1:25
1:1
10:1
kD
E-cadherin
Vimentin
β-actin
Slug
β-Tubulin
h
Overlay
AF488
E-cadherin
Vimentin
ConA-AF647
C. albicans
PBS

Figure 1. *Candida albicans* contributes to late-stage CRC progression.

(a,d) Representative histological images of tumor tissues stained by hematoxylin and eosin (H&E), antibodies against β-glucan. White arrowhead: positive area. **(b)** Abundance of C. albicans in different stages of colorectal adenocarcinoma (COAD). **(c)** Survival curve of patients in TCGA project with or without *C. albicans.* **(e)** Wound-healing assay for migration capability of PBS-, ***B. fragilis***-, *C. albicans*-, *B. fragilis* with *C. albican*-treated HCT116 cells. **(f)** Statistical analysis of gap size of different groups of CRC cells. **(g)** western blot to detect EMT proteins of HCT116 cells. Black arrowheads indicate positive staining sites. **(h)** Immunofluorescence images to detect EMT proteins of HCT116 cells. Black scale bars: 50 μm. White arrowhead: fungal hypha. The results shown here are expressed as the mean ± SEM. The following statistical analyses were performed: **(b)** Mann-Whitney-Wilcoxon test, **(c)**. Log-rank test, **(f)** one-way ANOVA followed by Tukey's multiple comparison test.

C. albicans induce hypoxia response pathway

To delineate the molecular mechanisms by which *C. albicans* facilitate cell migration, we conducted whole transcriptome sequencing (RNA-seq) on HCT116 cells co-cultured with *C. albicans*. As a result, we obtained significant up-regulation of 173 genes, which were potentially induced by *C. ablicans* infection (Figure 2a, Suppl. Table S1). Of note, various pro-tumor cytokines, including TNF, CXCL8, CCL22, and IL6 family gene, as well as their corresponding receptors, were found to be up-regulated (Figure 2a,k, Suppl. Table S2,S3), suggesting that *C. albicans* may actively contribute to the proinflammatory tumor microenvironment, thereby facilitating cancer progression[27]. Functional annotations of the up-regulated genes revealed enrichment in multiple metabolic pathways associated with tumor development, including hypoxia response, angiogenesis, epidermal growth factor signaling, and glucose metabolism (Suppl. Figure S2a and Table S4). Gene Set Enrichment Analysis (GSEA) further highlighted the up-regulation of the HIF-1α signaling pathway (Figure 2b, Suppl. Table S5). The up-regulation of key genes involved in HIF-1α signaling pathway, including HK2, LDHA, PDK1, and PFKFB1, were confirmed by qRT-PCR (Figure 2a,c, Suppl. Figure S2b). Moreover, treatment of HCT116 cells with i-mimosine, a compound that stabilizes HIF-1α, also significantly upregulated the expression of VEGFA, HK2, LDHA, PDK1, and PFKFB4 genes (Figure 2e, Suppl. Figure S2d). To reinforce the findings, we cultured HCT116 cells under hypoxia condition and performed RNA-seq, revealing that 83.8% (145 genes) of the genes up-regulated by *C. albicans* were also upregulated under hypoxia (Figure 2d).

With immunofluorescence staining, we observed the accumulation of HIF-1α in the nucleus and cytoplasm as early as 3 hours post-infection (Figure 2e). Western blots analysis further demonstrated that after *C. albicans* infection, HIF-1α increased in HCT116 and another two colorectal cell lines,

SW48 and Caco2, while the timing of upregulation varies among these three cell lines (Figure 2f, g). Angiogenesis, a critical process in cancer metastasis regulated by vascular endothelial growth factor (VEGF)[28], was also influenced by HIF-1α. qRT-PCR revealed an upregulation of VEGFA gene in the presence of *C. albicans* (Figure 2h). Western blot and immunofluorescence analyses further confirmed enhanced production of VEGFA protein in tumor cells co-cultured with *C. albicans* (Figure 2i-j). In addition to VEGFA, the expressions of chemokine C-X-C motif ligand 8 (CXCL8) and C-X-C motif chemokine receptor 4 (CXCR4) were both upregulated in tumor cells following exposure to *C. albicans* (Figure 2k, l). These findings suggested that *C. albicans* infection may modulate the tumor microenvironment by promoting angiogenesis. Collectively, these findings suggested that *C. albicans* infection induces the hypoxia response pathway in colorectal cancer cells, thereby facilitated angiogenesis and metabolism adaptation for cancer progression.

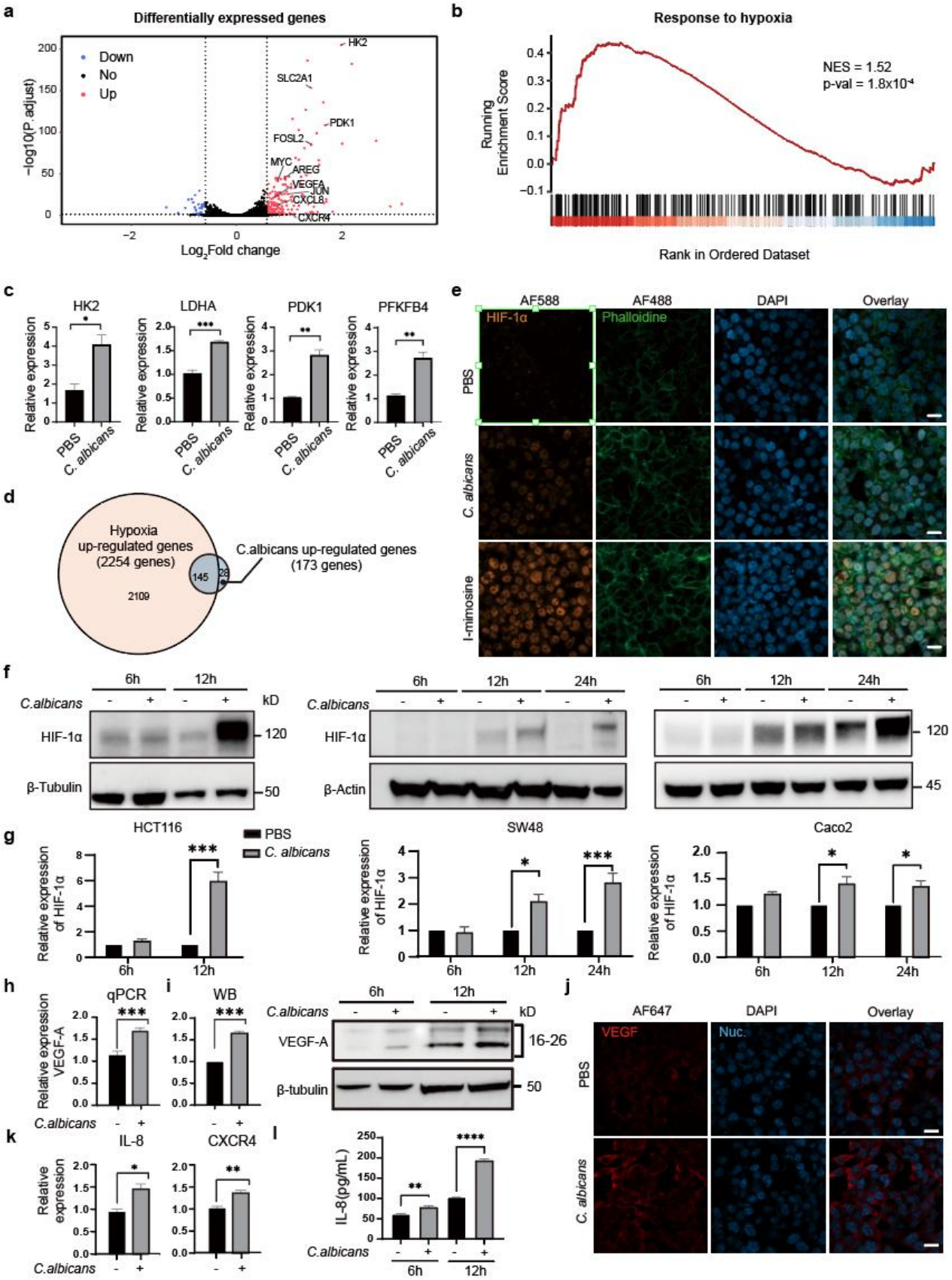
a
Differentially expressed genes
Down
No
Up
HK2
SLC2A1
PDK1
FOSL2
MYC
AREG
VEGFA
JUN
CXCL8
CXCR4
−log10(P.adjust)
Log2Fold change
b
Response to hypoxia
NES = 1.52
p-val = 1.8x10-4
Running Enrichment Score
Rank in Ordered Dataset
c
HK2
LDHA
PDK1
PFKFB4
Relative expression
PBS
C. albicans
d
Hypoxia up-regulated genes (2254 genes)
C.albicans up-regulated genes (173 genes)
145
28
2109
e
AF588
AF488
DAPI
Overlay
HIF-1α
Phalloidine
PBS
C. albicans
I-mimosine
f
6h
12h
24h
C.albicans
kD
HIF-1α
β-Tubulin
β-Actin
120
50
45
g
HCT116
SW48
Caco2
PBS
C. albicans
Relative expression of HIF-1α
h
qPCR
Relative expression VEGF-A
i
WB
VEGF-A
β-tubulin
16-26
j
AF647
DAPI
Overlay
VEGF
Nuc.
k
IL-8
CXCR4
Relative expression
l
IL-8(pg/mL)

129

130

Figure 2. *Candida albicans* induces hypoxia response pathway of colorectal cancer cells.

(a) Volcano plot shows the differentially expressed genes after C. albicans infection. Gene Ontology enrichment analysis in HCT116 cells treated with C. albicans for 24 hours compared with PBS treatment. **(b)** GSEA analysis was conducted to show the relationship between HIF-1α signaling pathway and C. albicans infection in HCT116 cells. **(c)** qRT-PCR was performed to detect expression of glycolysis genes in HCT116 cells cultured with C. albicans. **(d)** Venn diagram to show the intersection genes of HCT116 cells under hypoxia condition and C. albicans infection. **(e, f)** Immunofluorescence images **(e)** and Western blot to detect HIF-1α proteins of HCT116 cells, SW48 cells and Caco2 cells **(f)**. **(g)** Statistical analysis of HIF-1α protein level of different groups of CRC cells. One-way ANOVA followed by Tukey's multiple comparison test was used to assess statistical significance between samples from the same timepoint. **(h,i)** The expression of VEGFA detected by qPCR **(h)**, western blot **(i)** and Immunofluorescence **(j)** in HCT116 cells after C. albicans infection. **(k)** The expression of IL-8 and CXCR4 detected by qRT-PCR in HCT116 after C. albicans infection. **(l)** The concentration of IL-8 in cell culture supernatant. . The results shown here are expressed as the mean ± SEM. The following statistical analyses were performed: **(c, h, i, k)** unpaired Student's t-test. **(g, l)** one-way ANOVA followed by Tukey's multiple comparison test. *$p < 0.05$, **$p< 0.01$, ***$p< 0.001$.

C. albicans activated MAPK, c-Myc, and c-Jun to promote HIF-1α pathway

Besides the genes shown in Fig. 2e, the transcriptome data also uncovered a significant up-regulation of AP-1 (Activator protein 1) family and c-Myc genes in response to *C. albicans* infection, which we validated using qRT-PCR (Figure 3a). Considering the important roles of AP-1 in cell differentiation, migration, and proliferation[29], the expressions of c-Jun and c-Myc were further substantiated by Western blots. For c-Jun, expression levels increased at 12 hours post-infection in HCT116 cells and at 24 hours in SW48 cells following C. albicans infection (Figure 3b). Similarly, C. albicans infection significantly elevated the expression of c-Myc in both HCT116 and SW48 cancer cell lines at 12 hours post-infection (Figure 3c). Notably, a high multiplicity of infection (MOI) accelerated the cellular response, observable as early as 6 hours post-infection (Suppl. Figure S3a).

To determine the regulatory hierarchy in the up-regulations of c-Jun, c-Myc, and HIF-1α, we constructed HIF-1α knock down cell line and found that *C. albicans* still robustly upregulated c-Jun and c-Myc levels (Suppl. Figure S3b). Treatment of HCT116 cells with the c-Jun inhibitor SP600125 or knock down of c-Jun expression inhibited the cellular accumulation of HIF-1α after *C. albicans* infection (Figure 3d,e, Suppl. Figure S3c); similarly, treatment with the c-Myc inhibitor 10058-F4 or KJ-Pyr9 inhibited the cellular accumulation of HIF-1α after *C. albicans* infection (Figure 3f,g). The results suggested that c-Jun and c-Myc act upstream in the regulatory cascade leading to HIF-1α up-regulation. Moreover, treatment with i-mimosine caused upregulation of c-Jun but not c-Myc, implying a bidirectional regulation between c-Jun and HIF-1α (Suppl. Figure S3d). Together, these finding indicate that c-Myc and c-Jun collaborate to mediate the cell response to *C. albicans*.

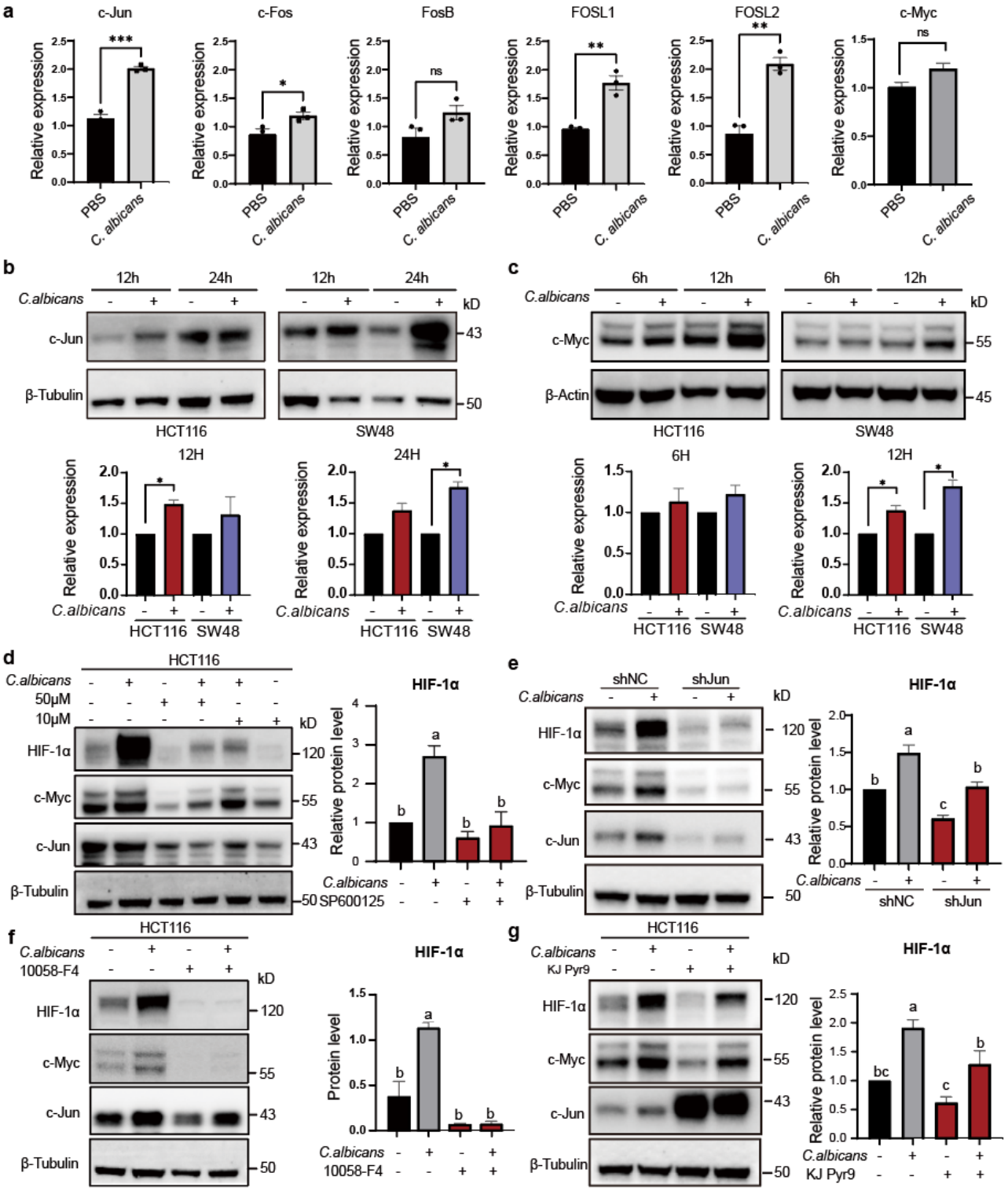

Figure 3. *Candida albicans* up-regulate the expression of transcription factor c-Myc, c-Jun to promote HIF-1α pathway. (a) qRT-PCR was performed to detect AP1 and c-Myc expression in HCT116 cells cultured with *C. albicans* for 12h. **(b, c)** Western blot to detect c-JUN **(b)** and c-Myc **(c)**

proteins of HCT116 cells and SW48 cells cultured with C. albicans for 12h and 24h. Right graph: Statistical analysis of c-JUN and c-Myc protein level of different groups of CRC cells. **(d)** Western blot to detect the HCT116 cell response after treated with c-Jun inhibitor SP600125 and *C. albicans* for 12h. **(e)** Western blot to detect the negative control and c-Jun knock down cell response after cultured with *C. albicans* for 12h. **(f-g)** Western blot to detect the HCT116 cell response after treated with c-Myc inhibitor inhibitor 10058-F4 **(f)** or KJ Pyr9 **(g)** and *C. albicans* for 12h. The following statistical analyses were performed: **(a)** Student's t-test. **(b-g)** one-way ANOVA followed by Tukey's multiple comparison test. *$p < 0.05$, **$p< 0.01$, ***$p< 0.001$.

EGFR and TLR are involved in C. albicans-mediated cell response

Next, we aimed to identify the cell membrane receptor responsible for C. albicans-mediated response. Specifically, genes related to the regulation of EGF-activated receptor activity were enriched following *C. albicans* infection (Suppl. Figure S2a). Indeed, both RNA-seq and qRT-PCR confirmed that *C. albicans* induced the expression of amphiregulin (AREG), a member of the epidermal growth factor (EGF) family and a known ligand of EGFR (Figure 4a). To explore the role of EGFR in the response to *C. albicans*, we treated HCT116 cells with the EGFR kinase inhibitor AG-1478. As a result, AG-1478 significantly reduced the activation of HIF-1α and c-Myc after *C. albicans* infection, indicating inhibition of the response triggered by *C. albicans* (Figure 4b-d); Given the complex regulatory network between HIF-1α, c-Jun, c-Myc and the mitogen-activated protein kinase (MAPK) pathway[30–36], we investigated the phosphorylation statuses of Erk and P38 (gene symbol: MAPK14), two important compartments of the EGFR-MAPK pathway. Western blots analysis revealed that *C. albicans* infection significantly increased the phosphorylation of Erk (Figure 4e), and treatment with the ERK inhibitor SCH772984 effectively suppressed the phosphorylation of Erk, consequently inhibiting the cellular responses triggered by *C. albicans*. On the other hand, phosphorylation of P38 remained unaffected after *C. albicans* infection, and treatment with the P38 inhibitor adezmapimod did not produce any significant inhibitory effect (Figure 4f), indicating a selective role of the ERK pathway in the cellular response to *C. albicans* infection.

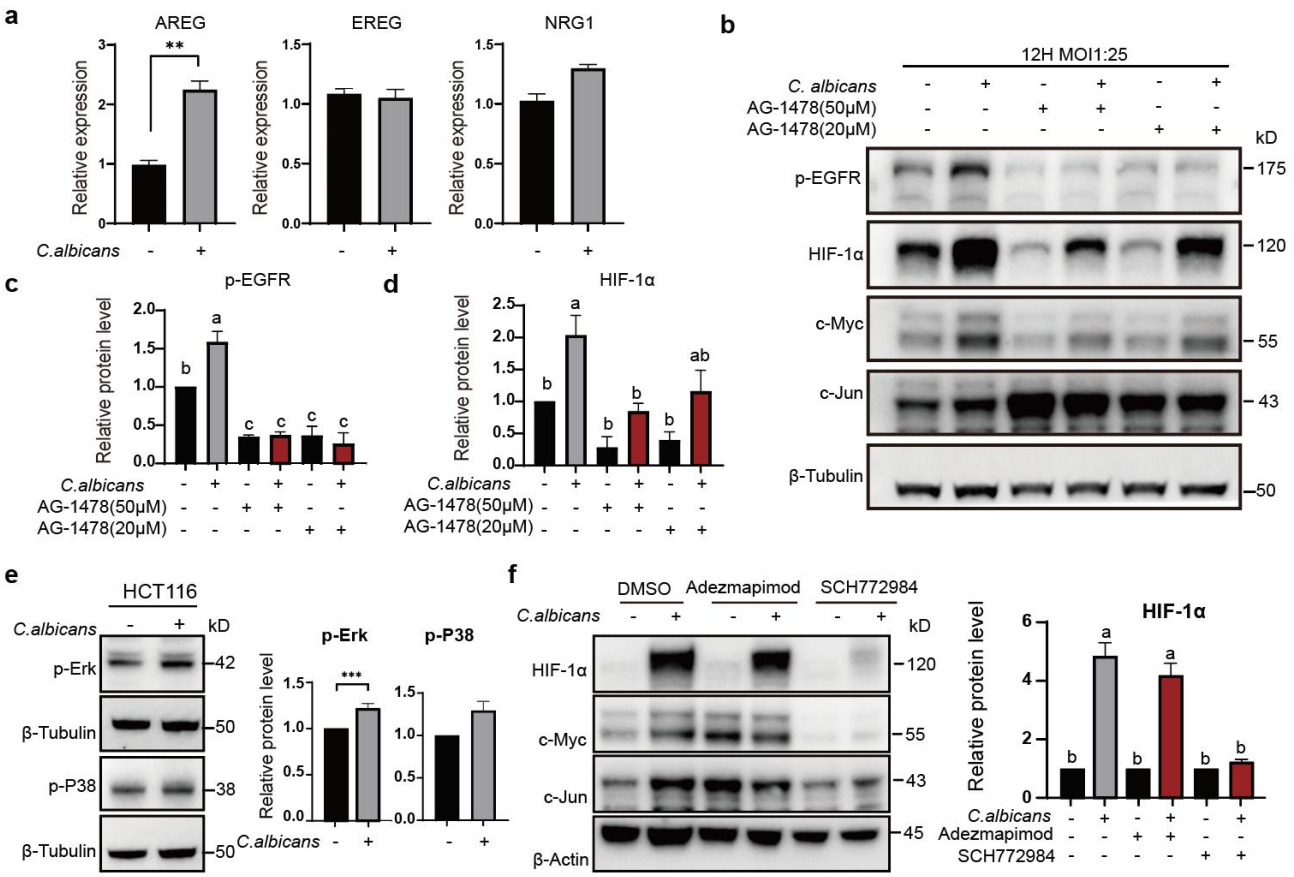

Figure 4. EGFR-ERK is involved in C. albicans-mediated cancer cell response.

(a) qRT-PCR was performed to detect expression of EGFR ligands in HCT116 cells cultured with C. albicans for 12h. **(b)** Western blot to detect proteins of HCT116 cells with AG-1478 added. **(c-d)** Statistical analysis of protein expression levels relative to the western blots in **(b)**. The following statistical analyses were performed: **(a)** Student's t-test. **(b-g)** one-way ANOVA followed by Tukey's multiple comparison test. *p < 0.05, **p< 0.01, ***p< 0.001.

Notably, despite treatment with AG1478, the levels of HIF-1α and c-MYC in *C. albicans*-infected cells remained significantly elevated compared to the uninfected control group (Figure 4b). We hypothesized that this residual effect might be due to the continued activation of cell surface Toll-like receptors (TLRs) or C-type lectin receptors (CLRs). Despite the low expression of TLR and CLR in HCT116 cells (Suppl. Figure S4a, S5a), we successfully generated stable knockdown cell lines for key receptors and pathways associated with fungal recognition, including TLR2, TLR6, TLR9, MYD88, Dectin-1, and SYK (Suppl. Figure S4b). Western blot results showed that neither the suppression of genes nor treatment with the TLR2 inhibitor MMG11 or the Dectin1 inhibitor laminarin impaired the cell responses following *C. albicans* infection (Figure 5a,b, Suppl. Figure S4b-e, S5b-d). However, when cells were treated with a combination of receptor inhibitors targeting both EGFR and TLR2, the activations of HIF-1α and c-MYC induced by *C. albicans* were completely suppressed (Figure 5c, d). Furthermore, we investigated the status of NF-κB, a key pathway responsive to TLR activation, after *C. albicans* infection[37–39]. Both immunofluorescence staining and western blot analyses revealed an increase in the phosphorylation level of p65 (gene symbol: RELA), a principal subunit of the NF-κB complex, following C. albicans infection. This led to nuclear translocation of p65, which modulated the expression of several downstream genes, including c-Jun and HIF-1α (Figure 5e-i). Additionally, combined EGFR and TLR2 inhibitors completely reversed the enhanced cell migration induced by *C. albicans* (Figure 5j-k). Collectively, the results suggested that *C. albicans* modulated the intracellular stability of HIF-1α by activating EGFR-ERK and TLR-NF-κB pathways, which further up-regulated a cohort of cellular transcription factors, including AP-1 components and c-Myc.

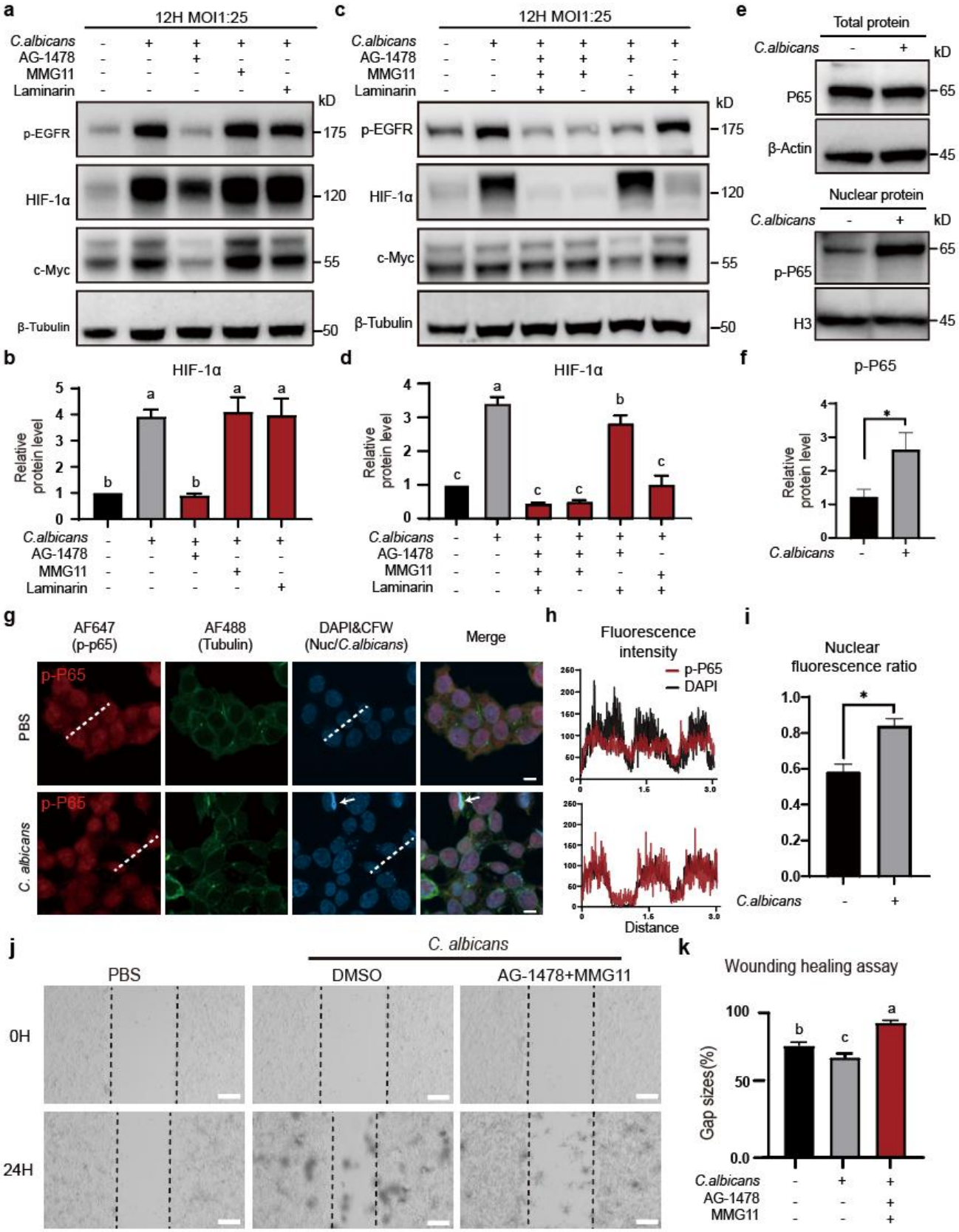
a
12H MOI1:25
C.albicans
AG-1478
MMG11
Laminarin
kD
p-EGFR
HIF-1α
c-Myc
β-Tubulin
175
120
55
50
c
12H MOI1:25
e
Total protein
P65
β-Actin
65
45
Nuclear protein
p-P65
H3
b
HIF-1α
Relative protein level
d
f
p-P65
g
AF647 (p-p65)
AF488 (Tubulin)
DAPI&CFW (Nuc/C.albicans)
Merge
PBS
C. albicans
h
Fluorescence intensity
DAPI
Distance
i
Nuclear fluorescence ratio
j
C. albicans
DMSO
AG-1478+MMG11
0H
24H
k
Wounding healing assay
Gap sizes(%)

Figure 5. *C. albicans* modulated the stability of HIF-1α by activating EGFR-ERK and TLR-NF-κB pathways.

(a, c) Western blot was performed to detect proteins level of HCT116 cells after different treatments. **(b, d)** Statistical analysis of HIF-1α protein levels relative to the Western blots in **(a, c)**. **(e)** Western blot to detect nuclear p-P65 proteins of HCT116 cells cultured with *C. albicans* for 12h. **(f)** Statistical analysis of p-P65 protein level of HCT116 cells cultured with *C. albicans* for 12h. **(g)** Immunofluorescence images to detect p-P65 proteins localization of HCT116 cells. **(h)** Relative signal intensities of the respective emission fluorescence along the lines drawn across the cells. **(i)** Statistical analysis of nuclear fluorescence ratio based on immunofluorescence images. **(j)** Representative pictures of wound-healing assay for migration capability of HCT116 cells after different treatments. **(k)** Statistical analysis of gap size of different groups. The following statistical analyses were performed: **(f, i)** unpaired Student's t-test. **(b, d, k)** one-way ANOVA followed by Tukey's multiple comparison test. $*p < 0.05$.

Candidalysin is essential for eliciting colorectal cancer cell response

To explore the virulence factor responsible for inducing cell responses, we co-cultured *C. albicans* with HCT116 cells and harvested *C. albicans* at various time points post-infection. qRT-PCR assays revealed that Als3, Hwp1, and Ece1 genes were significantly up-regulated in post-infection C. albicans (Figure 6a). Als3 and Hwp1 are known to be involved in the adhesion of *C. albicans* to epithelial cells, while Ece1 encodes the virulence factor candidalysin. Interestingly, the expression level of Ece1 showed a >1,000-fold increase (Figure 6a-b). In fact, during the early stages of mucosal surface infection by *C. albicans*, candidalysin is released into the invasion pocket created by the penetrating hyphae[21], where it activates danger-response and damage-protection pathways in host cells, including the activation of the epidermal growth factor receptor (EGFR) in epithelial cells and the NLRP3 inflammasome in macrophages[40,41]. Hence, these results suggest that candidalysin might play a critical role interacting with HCT116 cells.

To investigate the function of candidalysin during *C. albicans*-colon cell interaction, we generated an Ece1 knockout strain (termed as "Ece1Δ/Δ" hereafter) using the CRISPR/Cas9 system in *C. albicans* (Suppl. Figure S6a-b). This strain, which cannot synthesize candidalysin, was assessed for its ability to penetrate HCT116 cells using a differential fluorescence assay[21,42]. The Ece1Δ/Δ strain maintained the capacity to adhere to and enter HCT116 cells, similarly to the wild-type strain (Figure 6c-d). However, it failed to activate HIF-1α and c-Myc in the tumor cells (Figure 6e, g). In contrast, when HCT116 cells were treated with synthetic candidalysin, we observed a significant upregulation of c-Jun, c-Myc, and HIF-1α expression levels at 3μM for both uninfected HCT116 cells and those infected by ece1Δ/Δ strain *C. albicans* (Figure 6f, h). Moreover, treated with candidalysin activated MAPK pathway and showed promoted cell migration (Figure 6i, j). Together, these results indicate

that *C. albicans* regulates tumor cells through the secretion of candidalysin, which activates MAPK and hypoxia pathways to promote tumor cell migration.

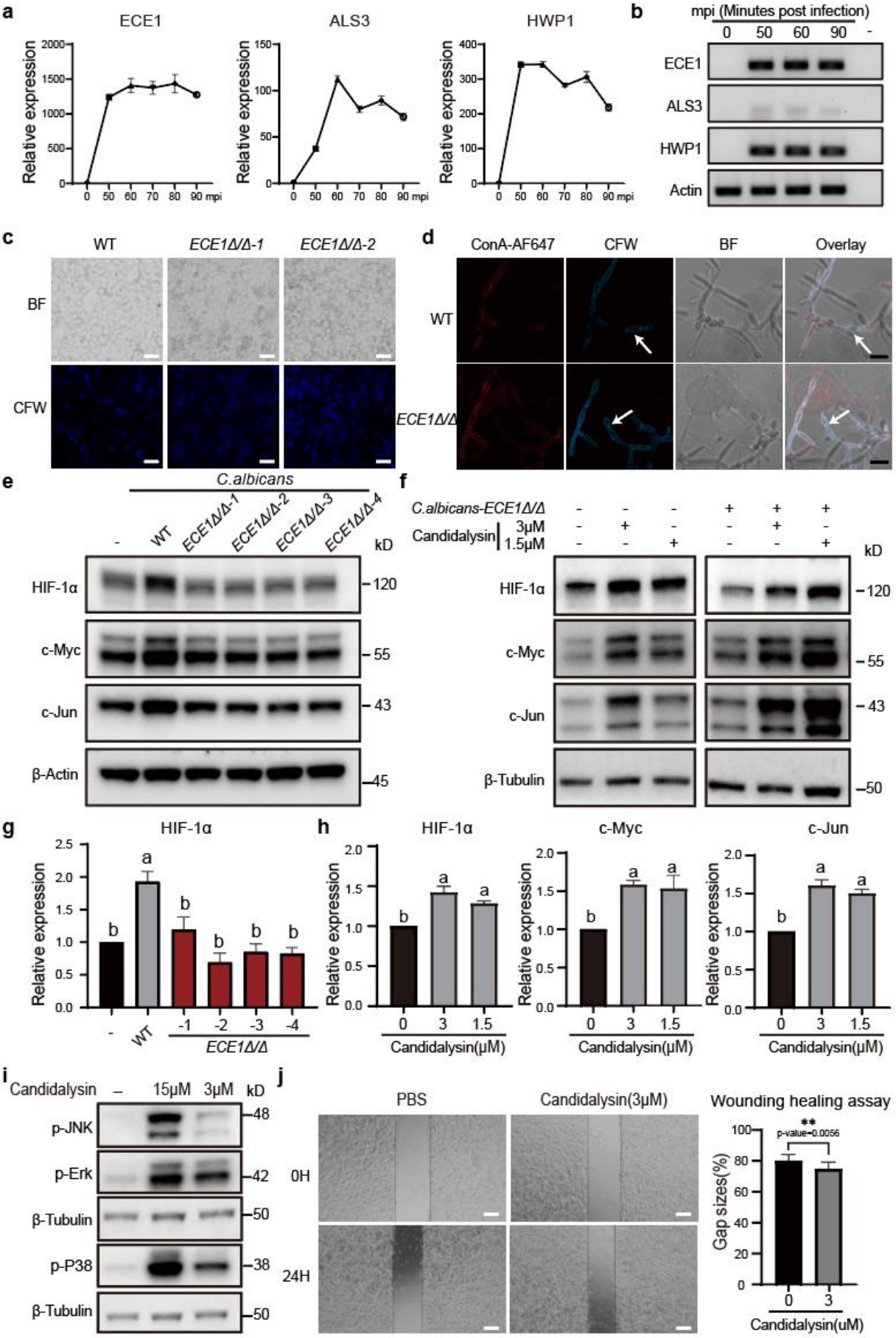
a
ECE1
ALS3
HWP1
Relative expression
0 50 60 70 80 90 mpi
b
mpi (Minutes post infection)
0 50 60 90 -
ECE1
ALS3
HWP1
Actin
c
WT
ECE1Δ/Δ-1
ECE1Δ/Δ-2
BF
CFW
d
ConA-AF647
CFW
BF
Overlay
WT
ECE1Δ/Δ
e
C.albicans
- WT ECE1Δ/Δ-1 ECE1Δ/Δ-2 ECE1Δ/Δ-3 ECE1Δ/Δ-4
kD
HIF-1α
c-Myc
c-Jun
β-Actin
120
55
43
45
f
C.albicans-ECE1Δ/Δ
Candidalysin 3μM
1.5μM
HIF-1α
c-Myc
c-Jun
β-Tubulin
120
55
43
50
g
HIF-1α
Relative expression
- WT -1 -2 -3 -4
ECE1Δ/Δ
h
HIF-1α
c-Myc
c-Jun
Candidalysin(μM)
i
Candidalysin – 15μM 3μM kD
p-JNK
p-Erk
β-Tubulin
p-P38
β-Tubulin
48
42
50
38
50
j
PBS
Candidalysin(3μM)
0H
24H
Wounding healing assay
**
p-value=0.0056
Gap sizes(%)
Candidalysin(uM)

Figure 6. Candidalysin is critical for eliciting colorectal cancer cells response.

(a, b) Chart showing the expression level of CaECE1, CaALS3 and CaHWP1 cultured with HCT116 cells from 0 to 90 mpi measured by qRT-PCR **(a)** and RT-PCR **(b)**. **(c)** Fluorescence staining of C. albicans wild-type and ece1Δ/Δ hyphae adherent to HCT116 cells. **(d)** Fluorescence staining of C. albicans wild-type and ece1Δ/Δ hyphae invading through HCT116 cells. White arrowheads indicate hyphal invading the cells. **(e)** Western blot to detect HIF-1α, c-JUN and c-Myc proteins of HCT116 cells cultured with C. albicans wild-type and ece1Δ/Δ for 12h. **(f)** Western blot analysis of HIF-1α, c-JUN, and c-Myc protein expression in HCT116 cells treated with synthetic candidalysin or the ece1Δ/Δ strain with added candidalysin. **(g-h)** Statistical analysis of protein expression levels relative to the Western blots in **(e)** and **(f)**, respectively. **(i)** Western blot to detect activation of MAPK pathway proteins of HCT116 cells with candidalysin added. **(j)** Wound-healing assay for migration capability of candidalysin-treated HCT116 cells. The following statistical analyses were performed: **(j)** unpaired Student's t-test. **(g, h)** One-way ANOVA followed by Tukey's multiple comparison test. $^{**}p < 0.01$.

C. albicans induce hypoxia responses in colon organoids and clinical specimens

To investigate whether *C. albicans* has the same effect on tumor samples, we collected three paired tumors and non-malignant colon tissues originating from CRC patients, which were isolated and cultured into organoids. After co-culturing *C. albicans* with the organoids for 12 hours, we also detected significant aggregation of HIF-1α in the cells, as evidenced by both Western blot and immunofluorescence staining, in both non-malignant intestinal organoids and tumor organoids (Figure 7a-c, Suppl. Figure S7a). Treatment of the organoids from colorectal cancer patients with c-Jun inhibitor SP600125 and c-Myc inhibitor 10058-F4 significantly suppressed the expression of HIF-1α (Figure 7d, Suppl. Figure S7b). Moreover, we observed that *C. albicans* hyphae penetrated the epithelium of colon organoids, reaching the lumen (Figure 7e). For the specimens analyzed in Figure 1a, we found higher levels of fungi near the colon mucosa in stage III samples compared to stage II sample, along with a notable aggregation of HIF-1α (Figure 7f, Suppl. Figure S8). Collectively, our findings suggest that *C. albicans* may contribute to the development of CRC by inducing HIF-1α aggregation in adjacent cells, thereby triggering hypoxia-related responses that create a microenvironment conducive to tumor progression.

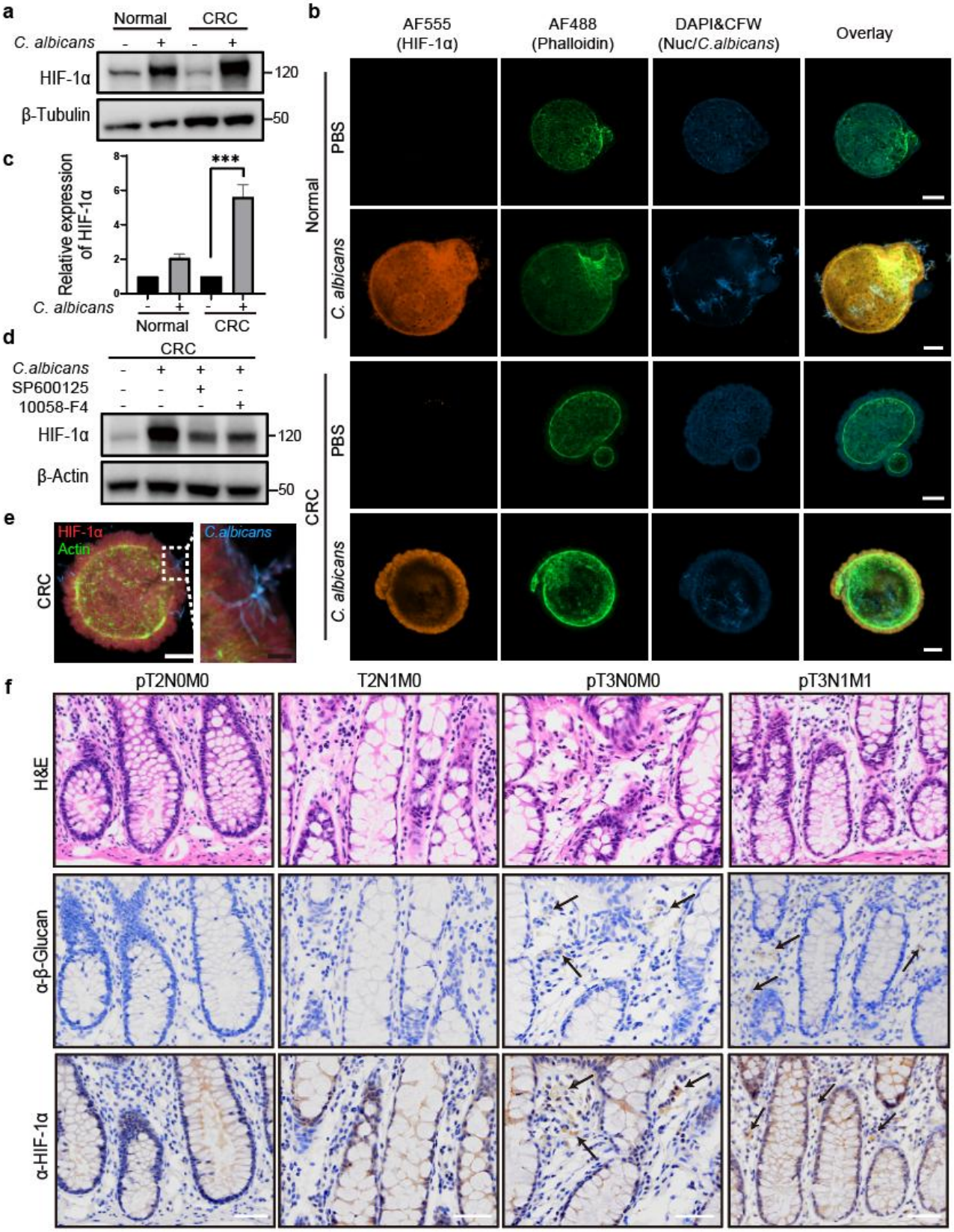
a
Normal
CRC
C. albicans
HIF-1α
β-Tubulin
120
50
b
AF555 (HIF-1α)
AF488 (Phalloidin)
DAPI&CFW (Nuc/C.albicans)
Overlay
Normal
CRC
PBS
C. albicans
c
Relative expression of HIF-1α
***
d
CRC
C.albicans
SP600125
10058-F4
HIF-1α
β-Actin
e
HIF-1α
Actin
C.albicans
f
pT2N0M0
T2N1M0
pT3N0M0
pT3N1M1
H&E
α-β-Glucan
α-HIF-1α

Figure 7. *Candida albicans* induces hypoxia response pathway of colon organoids and CRC samples.

Western blot **(a)** and Immunofluorescence images **(b)** and to detect HIF-1α proteins of normal and CRC organoids after C. albicans infection. **(c)** Statistical analysis of HIF-1α protein levels relative to the Western blots in **(a)**. **(d)** Western blot to detect the HCT116 cell response to c-Jun inhibitor SP600125 and c-Myc inhibitor 10058-F4. **(e)** Immunofluorescence images of CRC organoids after C. albicans infection. **(f)** Representative histological images of tumor tissues stained by hematoxylin and eosin (H&E), antibodies against β-glucan and HIF-1α. White bar=50μm, Black bar=10μm. One-way ANOVA followed by Tukey's multiple comparison test. ***$p < 0.001$.

Interactions between Candida and tumor cells exhibit both species and cellular specificity

Lastly, we explored the cellular responses of CRC cells to other fungus besides *C. albicans.* To do this, we conducted co-culture experiments using HCT116 cells and two other fungal species, *Saccharomyces cerevisiae* and *Candida tropicalis*, to assess their adhesive capacities and effects on cancer cells. As shown in Figure 8a,b, *C. tropicalis* and *S. cerevisiae* exhibited minimal adhesion to cancer cells (Figure 8a). Western blots were then performed to examine the subsequent effects of infection with these fungi, as well as a mixture of fungal cell wall polysaccharides and heat-killed Candida species. As a result, *C. albicans* and C. tropicalis exhibited the most potent ability to activate the hypoxia pathway, with *C. albicans* showing the strongest effect on the activation of c-Myc and c-Jun (Figure 8b). We hypothesized that the variations in cellular responses might be linked to the diversities of the Ece1 gene in the fungal genomes. Indeed, phylogenetic analysis revealed that evolutionarily, the Ece1 genes in various *Candida* species were highly conserved, whereas they differed significantly from other fungus. (Suppl. Figure S9). Of note, *C. tropicalis* did not express the ECE1 homolog after interaction with HCT116 cells for 1 hour (Suppl. Figure S10).

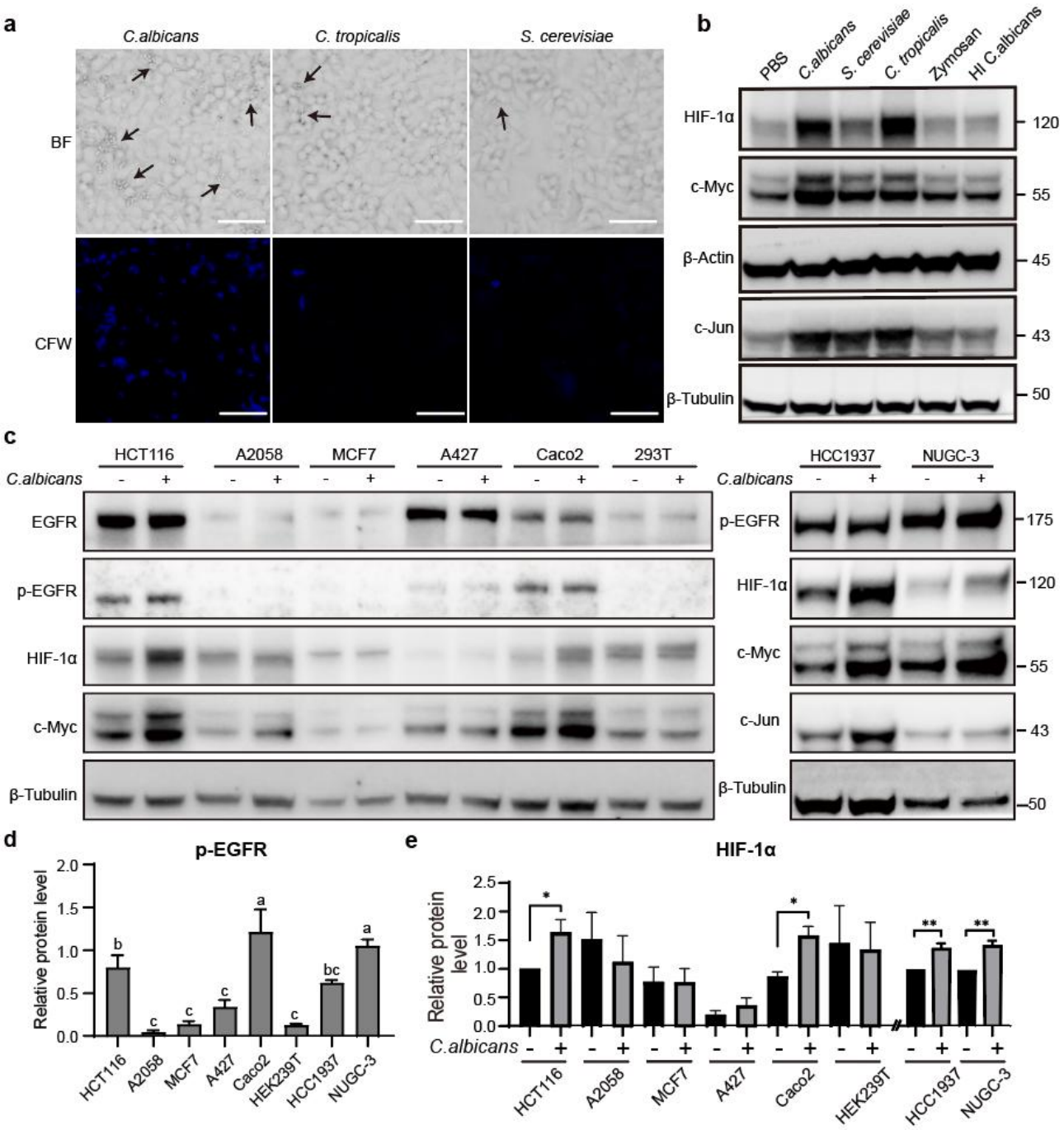

Figure 8. The interactions between Candida albicans and tumor cells exhibit both species and cellular specificity.

(a) Fluorescence staining of C. albicans, C. tropicalis and S. cerevisiae adherent to HCT116 cells. Black arrowheads indicate yeast or hyphal adherent to the cells. **(b)** Western blot was performed to detect proteins level of HCT116 cells after different treatments. **(c)** Western blot was performed to

detect the corresponding between p-EGFR and cell responses. **(d-e)** Statistical analysis of p-EGFR **(d)** and HIF-1α **(e)** protein levels relative to the Western blots in **(c)**. One-way ANOVA followed by Tukey's multiple comparison test. *$p < 0.05$, **$p < 0.01$, ***$p < 0.001$.

Additionally, we investigated the specificity of the response to *C. albicans* by co-culturing it with a variety of cancer cell lines. Intriguingly, we found that *C. albicans* not only activated the hypoxia pathway in CRC cells but also significantly induced similar responses in breast cancer cell line HCC1937 and the gastric carcinoma cell line NUGC-3. In contrast, *C. albicans* failed to elicit responses in melanoma cell line A2058, the breast ductal carcinoma cell line MCF7, and the human embryonic kidney cell line 293T (HEK293T) (Figure 8c). To explore the underlying mechanism responsible for these differences, we analyzed EGFR expression. As shown in Figure 8d, e, Suppl. Figure. S11, the results indicated a correlation between the expression and phosphorylation levels of EGFR and the phenotypic response to *C. albicans* infection. This was consistent with our earlier finding that *C. albicans* facilitates tumor cell migration through an EGFR-mediated pathway (Figure 4). Together, these findings suggest that candidalysin triggered EGFR/TLR2 - ERK/NF-κB - HIF-1α signaling pathway to induce hypoxia response, which promotes the progression of CRC (Figure 9).

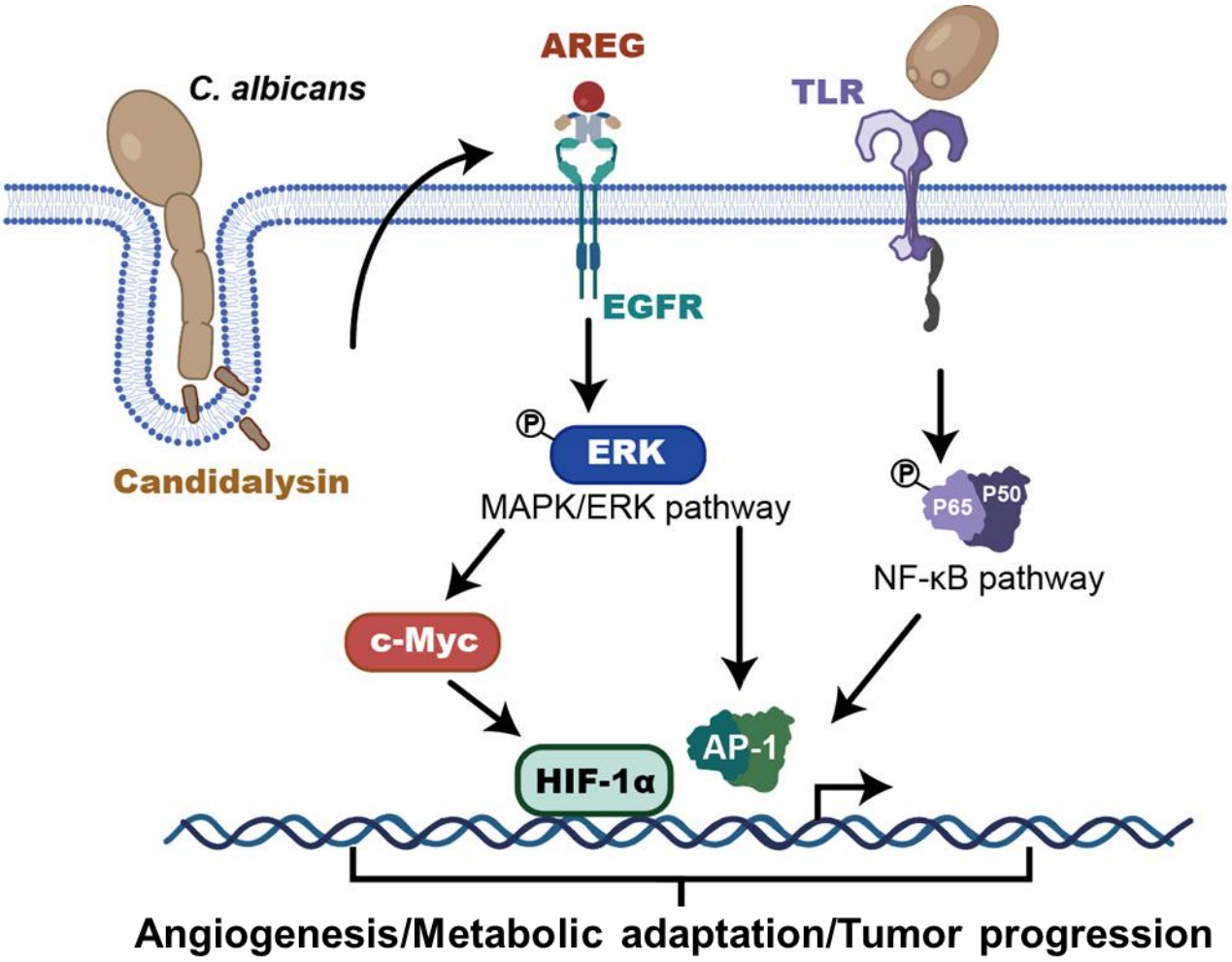

Figure 9. Schematic diagram of the *C. albicans* infection during colorectal cancer progression.

Discussion

Recent studies have sparked broad interest in the role of gut fungi, including *C. albicans*, in the development of various types of cancers[23,25,43]. In this study, we investigated the involvement of *C. albicans* in the progression of CRC. We demonstrated that after germinated in CRC, *C. albicans* secretes candidalysin, which induces a hypoxia response in the malignant cells through the EGFR/TLR2 - ERK/NF-κB - HIF-1α signaling pathway (Figure 9). The activation of hypoxia response pathway accelerates EMT and migration of tumor cells, which are key processes in cancer progression and metastasis. Hence, besides the interplay between *C. albicans* and tumor infiltrating immune cells (e.g., macrophages) reported in previous studies[25], our study identifies a novel mechanism by which *C. albicans* directly regulates the tumor cells to promote CRC progression.

Hypoxia is a hallmark of cancer, promoting angiogenesis and metastasis and resistance to therapy[44–46]. Under hypoxic conditions, metabolic shift in malignant cells enhance cell proliferation and invasion ability[47], as well as induce EMT and modulate the tumor microenvironment[48,49] to promote metastasis[50]. Interestingly, previous studies have shown that tumor-associated macrophages with *C. albicans* infection showed an increased glycolysis level through the HIF-1α-dependent pathway[25]. In our study, we demonstrated that in CRC, the hypoxia response activated by *C. albicans* relies on c-Jun and c-Myc, two key cancer-associated transcription factors that regulate cell progression, apoptosis, and cellular transformation[51,52]. This finding aligns with recent reports showing that c-Myc exerts considerable control over the levels and activity of HIF-1α[32,53]. Besides hypoxia, *C. albicans* also induced VEGFA expression (Figure 1), suggesting that the fungus may contribute to the vascularization of tumors, thereby facilitating nutrient supply and waste removal to boost tumor growth. Furthermore, activation of the NF-κB pathway by *C. albicans* suggested a potential role in

modulating the inflammatory response worthwhile for future investigations.

In addition, we demonstrated that candidalysin is the key molecular that triggers CRC cell response after *C. albicans* infection. Candidalysin is a peptide toxin secreted by the hyphal form of *C. albicans* during invasion, which helps *C. albicans* compete with bacterial species in the intestinal niche[54], and it is known to drive epithelial damage, immune activation, and phagocyte attraction[21,40,41,55]. Here we showed that candidalysin acted as a critical virulence factor that induces phosphorylation of EGFR to activate MAPK/ERK and downstream HIF-1α pathway. Recent studies have also shown that candidalysin can modulate multiple signaling pathways in various cancer types, e.g., activate the MAPK p38 mitogen-activated protein kinase through MAPK kinases and the kinase Src in oral cancer[55]. Together, these findings suggested that candidalysin, and its downstream EGFR, could serve as therapeutic targets to suppress *C. albicans*-induced metastasis-promoting responses for pharmacological interventions. Moreover, the species- and cell-specificity of the interactions between *Candida* species and tumor cells (Figure 7) highlights the need for a nuanced understanding of the tumor microbiome. Interestingly, *C. tropicalis* are able to induce HIF-1α accumulation, while it does not secret candidalysin (Figure 7b, Suppl. Figure S12)[56]. In fact, previous studies reported that *C. tropicalis* induce PKM2 phosphorylation which then upregulates HIF-1α pathway[57], suggesting high diversity of fungus-tumor interplays that requires more explorations.

In conclusion, this study uncovered the molecular responses induced by *C. albicans* to promote CRC progression. The ability of *C. albicans* to modulate CRC cells has important implications for our understanding in the roles of microbiome during cancer progression.

Methods

Ethics approval and cell culture

This study had been approved by the Ethics Committee of Shenzhen Bay Laboratory, Ethics Committee of Southern University of Science and Technology, and Ethics Committee of The Seventh Affiliated Hospital, Sun Yat-Sen University. Clinical colon tumor samples were collected from Southern University of Science and Technology Hospital, and The Seventh Affiliated Hospital, Sun Yat-Sen University with written informed consents. The human CRC cell line HCT116 is cultured in RPMI 1640 Medium (Thermo, #C11875500BT), supplemented with 10% Fetal Bovine Serum (FBS) (Sigma-Aldrich, #F0193), at 37°C in a humidified incubator with an atmosphere of 5% CO2. The human CRC cell lines SW48 and Caco2, breast cancer cell line MCF7, melanoma cell line A2058, and embryonic kidney cells HEK293T are grown in Dulbecco's Modified Eagle Medium (DMEM) (Thermo, #C11995500BT) supplemented with 10% FBS, under the same conditions. *C. albicans*, *C. tropicalis,* and *S. cerevisiae* were grown on YPD (Yeast Peptone Dextrose) agar plate (HKM, #21100). Prior to infection, a single colony was inoculated into 4 ml YPD liquid medium and incubated overnight at 30°C in a high-humidity environment. Bacteroides fragilis was cultured on columbia blood agar plate (HKM, #CP0160) and inoculated with a single colony into 5 ml BHI broth, supplemented with 25μg/ml hemin chloride and 10μg/ml vitamin K1(HKM, #SR0300). Cultures were maintained in an anaerobic chamber at 37°C.

TCGA data and survival analysis

The abundance of *C. albicans* in colon adenocarcinoma samples in The Cancer Genome Atlas (TCGA) was collected from Narunsky-Haziza et al. that characterized fungal populations across multiple cancer

types[58]. Survival analysis was performed in the "survival" package in R.

Co-culture of cells and strains

For co-culture of cell line and strains, 1×10^6 cells were grown to confluence on 6-well plate. Before co-culture, the medium was replaced with 2 ml RPMI 1640 without FBS and supplemented with the strains, then incubated for 6 or 12 hours at 37 °C/5% CO2. For co-culture of organoids and *C. albicans*, approximately 200 colon organoids (~5×10^5 cells) were harvest from a 12-well plate. Organoids were gently washed with 1 mL of DMEM medium without FBS, then the DMEM was aspirated and replaced with 1 mL of the organoid culture medium. The medium was then replaced with 1 ml serum-free medium supplemented with *C. albicans* and incubated for 12 hours at 37 °C/5% CO_2.

Cell migration assay

Cell migration was assessed using a wound-healing assay. Briefly, HCT116 cells were seeded in 6-well culture plates to reach approximately 90% confluence. A wound was introduced by manually scraping. Following the initial wound creation, cells were washed with phosphate-buffered saline (PBS) to remove debris and 2 ml serum-free medium supplemented with the strains was added. Cells were then incubated at 37°C in a CO2 incubator for 24 hours. Images of the wounded area were captured at 0 and 24 hours, and the gap sizes were quantified by measuring the wound area using ImageJ software. The relative gap size was calculated by comparing the wound area at 24 hours to the initial wound size.

RNA extraction and real-time PCR

Total RNA was isolated from cultured tumor cells using a commercial kit (Zymo, #R2052), followed

by quantification and purity assessment with nanodrop. 1μg of total RNA were treated with DNase to eliminate DNA contamination and then converted to cDNA using a high-capacity cDNA synthesis kit (Vazyme, #R333-01). For quantitative Real-Time PCR (qPCR), gene-specific primers were used in a SYBR Green-based qPCR assay to quantify the expression levels of target genes (Vazyme, #Q712-02). The qPCR cycling conditions included an initial denaturation step, followed by 40 cycles of amplification. Relative gene expression was determined using the $2^{-\Delta\Delta Ct}$ method with β-actin served as endogenous control for normalization. The DNA primers were listed in Suppl. Table S6.

Protein extraction and western blots

Tumor cells were lysed in a radioimmunoprecipitation assay (RIPA) buffer (Beyotime, #P0013) containing protease and phosphatase inhibitors (Selleck, #B14001, #B15001). The lysate was centrifuged, and the supernatant containing the total protein was collected. Protein concentration was determined using the detergent compatible bradford protein assay kit (Beyotime, #P0006C) with bovine serum albumin (BSA) used for standard curve construction. For western blot analysis, 10μg protein samples were separated by sodium dodecyl sulfate-polyacrylamide gel electrophoresis (SDS-PAGE) and then transferred to a polyvinylidene fluoride (PVDF) membrane. After blocking with 5% non-fat dry milk for one hour, the membrane was incubated with a primary antibody at 4°C overnight, followed by a horseradish peroxidase (HRP)-conjugated secondary antibody (1:5000). Protein bands were visualized using an SuperFemto ECL Chemiluminescence Kit (Vazyme, # E423-01). Images were analyzed using ImageJ software. Human α-actin and β-tubulin were used as a loading control. The antibodies and dilutions were listed in Suppl. Table S7.

ELISA to detect the IL-8 concentration

After completing the co-culture experiments, culture supernatants were collected and stored at −80 °C for future analysis. The assays were conducted according to the manufacturers' protocols (ELabscience, #E-OSEL-H0014). In brief, IL-8 was captured by antibodies pre-coated on 96-well plates. Subsequently, biotinylated detection antibodies were applied to the wells, followed by the addition of a streptavidin-horseradish peroxidase (HRP) complex. The presence of the IL-8 was then visualized by adding a substrate solution, and the absorbance was measured at approximately 450 nm using a spectrophotometer.

Whole transcriptome sequencing and data analysis

For RNA sequencing, total RNA was extracted from tumor cells using column-based purification method (Zymo, #R2052) and analyzed for quality on an Agilent 2100 Bioanalyzer. Ribosomal RNA (rRNA) was depleted using a commercially available kit (Vazyme, #N406-01), which selectively removes rRNA and enriches the mRNA fraction. The rRNA-depleted RNA was fragmented and used to construct a cDNA library following a protocol provided by VAHTS Universal V8 RNA-seq Library Prep Kit for MGI (Vazyme, #NRM605-01). The cDNA library was amplified using PCR and analyzed for size distribution on an Agilent 4200 TapeStation System, then subjected to a circularization process to form a concatemers of the cDNA fragments (Vazyme, #NM201-01). After quantified using a Qubit fluorometer, the circularized library was loaded onto a sequencing flow cell and sequenced on a MGISEQ-2000 sequencer (MGI) in paired-end 150 bp mode.

RNA-seq data analysis was analyzed as in our previous study[59]. Briefly, raw sequencing reads were first subjected to adapter trimming and low-quality base removal with Ktrim software (version

1.5.0)[60], and then aligned to the human reference genome (NCBI GRCh38) with STAR software (version 2.7.9a)[61]. Gene expression quantifications were conducted using FeatureCounts software (version 2.0.3)[62]. Subsequently, differential gene expression analysis was performed with DESeq2 (version 1.26.0)[63]. Gene Ontology (GO) enrichment analysis was conducted with ClusterProfiler (version 4.12.6)[64]. Gene Set Enrichment Analysis (GSEA) was applied to identify coordinated expression changes within biological pathways[65].

Immunofluorescence staining

For cell immunofluorescence (IF) staining, HCT116 cells were evenly distributed onto 8-well chamber slides at a density of 10^5 cells per well. After reaching ~90% confluence, cells were washed with phosphate-buffered saline (PBS) and 200ul serum-free medium supplemented with the 10^5 *C. albicans* (MOI 1:1) was added. After 3 hours of culture in a humidified incubator (37°C/5% CO2), slides were fixed with 4% paraformaldehyde for 15 minutes at room temperature, followed by permeabilized with 0.1% Triton X-100 in PBS for 10 minutes. Non-specific binding was blocked with 5% bovine serum albumin (BSA) in PBS for 1 hour at room temperature. Cells were incubated with the primary antibody overnight at 4°C in a humidified chamber. After washing with PBS, the slides were incubated with a fluorochrome-conjugated secondary antibody (1:1000 dilution) and for 1 hour at room temperature in the dark. *C. albicans* were marked with Concanavalin A-Alexa Fluor 647 or Calcofluor White. Finally, the slides were mounted using an antifade mounting medium with DAPI (Beyotime, #P0131).

For organoids staining, uninfected and infected organoids were fixed in 4% paraformaldehyde in 100 mM PBS for 1 hour, washed with PBS with 100 mM glycine, permeabilized in 0.5% Triton X-100 in PBS for 1 hour, then incubated in staining buffer (4% BSA, 0.05% Tween-20 in PBS pH 7.4,

512 10% goat/donkey serum) for 4 hours, followed by incubation with primary antibody for 24 hours at
513 4°C. After washing with PBST (PBS with 0.05% Tween-20), incubated with fluorescent secondary
514 antibodies, phalloidin and DAPI, for 4 h at room temperature. Following additional washes, whole
515 mounts were submerged in antifade mounting medium (Beyotime, #P0126). Images were captured
516 using Zeiss LSM900 confocal microscope (Carl Zeiss) fitted with a 63× oil immersion objective or
517 10× objective.

518

519 *Construction of stable cell lines*

520 Lentiviral particles were produced by co-transfecting 293T cells with the shRNA expression vector
521 (pLKO-shRNA-EGFP vector) along with packaging (psPAX2) and envelope (pMD2.G) plasmids,
522 using Lipofectamine 3000 Transfection Reagent (Thermos, #L3000015). The culture medium was
523 replaced 24 hours post-transfection, and the lentiviral supernatant was collected 48 and 72 hours,
524 filtered through a 0.45 μm filter. After HCT116 cells reach approximately 70% confluence, lentiviral
525 particles were added to the cells in the presence of polybrene (5 μg/mL) to enhance infection efficiency.
526 The cells were then incubated at 37°C for 24 hours. Stably transfected cells were selected using a
527 Beckman CytoFLEX SRT Benchtop Cell Sorter. The efficiency of shRNA-mediated knockdown was
528 validated at the mRNA levels. The DNA primers for plasmid construction were listed in Table S1.

529

530 *Generation of C. albicans mutant strains*

531 ECE deletion was performed according to the method descripted by Nguyen. Briefly, Guide RNAs
532 (gRNAs) were designed using the CRISPOR online website (http://crispor.tefor.net/). The gRNA
533 sequences were integrated with gRNA expression cassettes by cloning-free stitching PCR. The Cas9

expression cassette was amplified from vector pADH137. The 500bp upstream and downstream sequences of ECE1 were fused with mCherry by fusion PCR. Cas9 cassette, gRNA cassette and donor DNA were transformed into the competent cells of *C. albicans* using the lithium acetate transformation method. Transformants were selected on YPD agar plates containing nourseothricin to isolate stably integrated cells. Single colonies from the selection plates were picked and grown in liquid YPD medium. Genomic DNA was extracted and the ECE1 locus modification was PCR amplified using primers flanking and inner of the target site.

Tissue processing and organoid culture

Adjacent normal and tumor tissues were isolated from the resected colon segments. Healthy crypts and tumor epithelium was isolated essentially as described by Sato et al[66]. Organoids from adjacent colonic tissues were cultured in optimized human intestinal organoid medium[67]. The composition of medium is: advanced DMEM/F12 basal culture medium with 1% HEPES, 1% GlutaMAX, 1% Penicillin-Streptomycin, 10 ng/ml Wnt, 100 ng/ml R-Spondin, 100 ng/ml Noggin, 1× B27, 1,25 mM n-Acetyl Cysteine, 50 ng/ml human EGF, 5 uM A83-01, 3 uM SB202190, and 100 μg/ml Primocin. Tumor organoids were cultured with organoid medium minus Wnt and R-Spondin for the selection of organoids with intrinsic Wnt signaling activation. Organoids were split once a week and medium were refreshed every three days.

H&E and immunohistochemistry staining

Tissue specimens collected from colorectal cancer patients were fixed in freshly prepared 4% paraformaldehyde at 4 °C for 24 hours. After fixation, the tissues were dehydrated, embedded, and

sectioned. Hematoxylin and eosin (H&E) staining and immunohistochemistry (IHC) were performed using standard procedures. H&E staining involved the use of hematoxylin and eosin dyes. For immunohistochemistry (IHC), specific primary antibodies targeting β-1,3-glucan (1:100) and HIF-1α (1:200) were applied to detect the presence and localization of these markers within the tissue sections. The stained slides were scanned using the SLIDEVIEW VS200 system (Olympus), and images were processed using OlyVIA software (Olympus).

Statistical analysis

All experiments were performed in triplicate, and the data is presented as the mean ± standard error of the mean (SEM). Statistical analysis was conducted using unpaired t-test and a one-way ANOVA followed by a post-hoc Tukey test to determine the significance of differences between two groups and more than two groups respectively.

Declaration of interests

The authors declare no conflict of interests.

Acknowledgements

This work was supported by National Key R&D Program of China (2022YFA0912700), China Postdoctoral Science Foundation (2023M742421), Shenzhen Bay Scholar Fellowship (to C.D. and K.S.), and Major Program of Shenzhen Bay Laboratory (S241101004). We'd like to thank Ms. Qi Wang for technical assistance, SZBL Bioimaging Core, and SZBL High Performance Computing and Informatics Core for technical supports.

Author contributions

Conception and design: W.W., K.S.; Study supervision: W.W., G.H., K.S.; Development of methodology: W.W., H.L.; Patient recruitment and clinical data analysis: C.D., N.L.; Cell culture and experiments: W.W., H.L., Y.M.; Acquisition of data: all authors; Analysis and interpretation of data: all authors; Writing the manuscript: W.W., K.S.; Review and edit of the manuscript: W.W., Y.Z., G.H., K.S.

Reference

1. Siegel, R. L., Wagle, N. S., Cercek, A., Smith, R. A. & Jemal, A. Colorectal cancer statistics, 2023. *CA A Cancer J Clinicians* **73**, 233–254 (2023).
2. Piawah, S. & Venook, A. P. Targeted therapy for colorectal cancer metastases: A review of current methods of molecularly targeted therapy and the use of tumor biomarkers in the treatment of metastatic colorectal cancer. *Cancer* **125**, 4139–4147 (2019).
3. Yang, Y. *et al.* Fusobacterium nucleatum Increases Proliferation of Colorectal Cancer Cells and Tumor Development in Mice by Activating TLR4 Signaling to NFκB, Upregulating Expression of microRNA-21. *Gastroenterology* **152**, 851-866.e24 (2017).
4. Yu, T. *et al.* Fusobacterium nucleatum Promotes Chemoresistance to Colorectal Cancer by Modulating Autophagy. *Cell* **170**, 548-563.e16 (2017).
5. Gur, C. *et al.* Binding of the Fap2 Protein of Fusobacterium nucleatum to Human Inhibitory Receptor TIGIT Protects Tumors from Immune Cell Attack. *Immunity* **42**, 344–355 (2015).
6. Abed, J. *et al.* Fap2 Mediates Fusobacterium nucleatum Colorectal Adenocarcinoma Enrichment by Binding to Tumor-Expressed Gal-GalNAc. *Cell Host & Microbe* **20**, 215–225 (2016).
7. Garrett, W. S. The gut microbiota and colon cancer. *Science* **364**, 1133–1135 (2019).
8. Liu, Q.-Q. *et al.* Enterotoxigenic Bacteroides fragilis induces the stemness in colorectal cancer via upregulating histone demethylase JMJD2B. *Gut Microbes* **12**, 1788900 (2020).
9. Sepich-Poore, G. D. *et al.* The microbiome and human cancer. *Science* **371**, eabc4552 (2021).
10. Wang, X. *et al.* Candida albicans accelerates atherosclerosis by activating intestinal hypoxia-inducible factor2α signaling. *Cell Host & Microbe* S1931312824001379 (2024) doi:10.1016/j.chom.2024.04.017.
11. Benakis, C. *et al.* Commensal microbiota affects ischemic stroke outcome by regulating intestinal γδ T cells. *Nat Med* **22**, 516–523 (2016).
12. Buffington, S. A. *et al.* Dissecting the contribution of host genetics and the microbiome in complex behaviors. *Cell* **184**, 1740-1756.e16 (2021).
13. Alam, A. *et al.* Fungal mycobiome drives IL-33 secretion and type 2 immunity in pancreatic cancer. *Cancer Cell* **40**, 153-167.e11 (2022).
14. Aykut, B. *et al.* The fungal mycobiome promotes pancreatic oncogenesis via activation of MBL. *Nature* **574**, 264–267 (2019).

15. Wang, T. *et al.* The Adaptor Protein CARD9 Protects against Colon Cancer by Restricting Mycobiota-Mediated Expansion of Myeloid-Derived Suppressor Cells. *Immunity* **49**, 504-514.e4 (2018).
16. Malik, A. *et al.* SYK-CARD9 Signaling Axis Promotes Gut Fungi-Mediated Inflammasome Activation to Restrict Colitis and Colon Cancer. *Immunity* **49**, 515-530.e5 (2018).
17. Pappas, P. G., Lionakis, M. S., Arendrup, M. C., Ostrosky-Zeichner, L. & Kullberg, B. J. Invasive candidiasis. *Nat Rev Dis Primers* **4**, 1–20 (2018).
18. Phan, Q. T. *et al.* Als3 Is a Candida albicans Invasin That Binds to Cadherins and Induces Endocytosis by Host Cells. *PLOS Biology* **5**, e64 (2007).
19. Naglik, J. R., Richardson, J. P. & Moyes, D. L. Candida albicans Pathogenicity and Epithelial Immunity. *PLOS Pathogens* **10**, e1004257 (2014).
20. Phan, Q. T. *et al.* Candida albicans stimulates formation of a multi-receptor complex that mediates epithelial cell invasion during oropharyngeal infection. *PLOS Pathogens* **19**, e1011579 (2023).
21. Moyes, D. L. *et al.* Candidalysin is a fungal peptide toxin critical for mucosal infection. *Nature* **532**, 64–68 (2016).
22. Dohlman, A. B. *et al.* A pan-cancer mycobiome analysis reveals fungal involvement in gastrointestinal and lung tumors. *Cell* **185**, 3807-3822.e12 (2022).
23. Vadovics, M. *et al.* Candida albicans Enhances the Progression of Oral Squamous Cell Carcinoma In Vitro and In Vivo. *mBio* **13**, e03144-21 (2022).
24. Yang, Z., Zhang, S., Ji, N., Li, J. & Chen, Q. The evil companion of OSCC: Candida albicans. *Oral Diseases* **00**, 1–14 (2023).
25. Zhu, Y. *et al.* Fungal-induced glycolysis in macrophages promotes colon cancer by enhancing innate lymphoid cell secretion of IL-22. *The EMBO Journal* **40**, e105320 (2021).
26. Cancer Genome Atlas Network. Comprehensive molecular characterization of human colon and rectal cancer. *Nature* **487**, 330–337 (2012).
27. Bhat, A. A. *et al.* Cytokine- and chemokine-induced inflammatory colorectal tumor microenvironment: Emerging avenue for targeted therapy. *Cancer Communications* **42**, 689–715 (2022).
28. Pérez-Gutiérrez, L. & Ferrara, N. Biology and therapeutic targeting of vascular endothelial growth factor A. *Nat Rev Mol Cell Biol* **24**, 816–834 (2023).
29. Shaulian, E. & Karin, M. AP-1 as a regulator of cell life and death. *Nat Cell Biol* **4**, E131-136 (2002).
30. Pulverer, B. J., Kyriakis, J. M., Avruch, J., Nikolakaki, E. & Woodgett, J. R. Phosphorylation of c-jun mediated by MAP kinases. *Nature* **353**, 670–674 (1991).
31. Doe, M. R., Ascano, J. M., Kaur, M. & Cole, M. D. Myc Posttranscriptionally Induces HIF1 Protein and Target Gene Expression in Normal and Cancer Cells. *Cancer Research* **72**, 949–957 (2012).
32. Chen, C. *et al.* c-Myc enhances colon cancer cell-mediated angiogenesis through the regulation of HIF-1α. *Biochemical and Biophysical Research Communications* **430**, 505–511 (2013).
33. Yu, B. *et al.* c-Jun Protects Hypoxia-Inducible Factor-1α from Degradation via Its Oxygen-Dependent Degradation Domain in a Nontranscriptional Manner. *Cancer Research* **69**, 7704–7712 (2009).
34. Alfranca, A. *et al.* c-Jun and Hypoxia-Inducible Factor 1 Functionally Cooperate in Hypoxia-Induced Gene Transcription. *Mol Cell Biol* **22**, 12–22 (2002).
35. Lee, S. H. *et al.* ERK activation drives intestinal tumorigenesis in Apcmin/+ mice. *Nat Med* **16**, 665–670 (2010).
36. Sears, R. *et al.* Multiple Ras-dependent phosphorylation pathways regulate Myc protein stability. *Genes Dev.* **14**, 2501–2514 (2000).
37. Duyao, M. P., Buckler, A. J. & Sonenshein, G. E. Interaction of an NF-kappa B-like factor with a site upstream of the c-myc promoter. *Proceedings of the National Academy of Sciences* **87**, 4727–4731 (1990).

38. Rius, J. *et al.* NF-κB links innate immunity to the hypoxic response through transcriptional regulation of HIF-1α. *Nature* **453**, 807–811 (2008).
39. Oeckinghaus, A., Hayden, M. S. & Ghosh, S. Crosstalk in NF-κB signaling pathways. *Nat Immunol* **12**, 695–708 (2011).
40. Ho, J. *et al.* Candidalysin activates innate epithelial immune responses via epidermal growth factor receptor. *Nat Commun* **10**, 2297 (2019).
41. Kasper, L. *et al.* The fungal peptide toxin Candidalysin activates the NLRP3 inflammasome and causes cytolysis in mononuclear phagocytes. *Nat Commun* **9**, 4260 (2018).
42. Nguyen, N., Quail, M. M. F. & Hernday, A. D. An Efficient, Rapid, and Recyclable System for CRISPR-Mediated Genome Editing in Candida albicans. *mSphere* **2**, 10.1128/mspheredirect.00149-17 (2017).
43. Ho, J. *et al.* Candida albicans and candidalysin in inflammatory disorders and cancer. *Immunology* **162**, 11–16 (2021).
44. Chen, Z., Han, F., Du, Y., Shi, H. & Zhou, W. Hypoxic microenvironment in cancer: molecular mechanisms and therapeutic interventions. *Sig Transduct Target Ther* **8**, 1–23 (2023).
45. Ye, Y. *et al.* Characterization of hypoxia-associated molecular features to aid hypoxia-targeted therapy. *Nat Metab* **1**, 431–444 (2019).
46. Wilson, W. R. & Hay, M. P. Targeting hypoxia in cancer therapy. *Nat Rev Cancer* **11**, 393–410 (2011).
47. Paredes, F., Williams, H. C. & Martin, A. S. Metabolic adaptation in hypoxia and cancer. *Cancer Lett* **502**, 133–142 (2021).
48. Wang, Y. *et al.* Granulocytic Myeloid-Derived Suppressor Cells Promote the Stemness of Colorectal Cancer Cells through Exosomal S100A9. *Advanced Science* **6**, 1901278 (2019).
49. Chaturvedi, P., Gilkes, D. M., Takano, N. & Semenza, G. L. Hypoxia-inducible factor-dependent signaling between triple-negative breast cancer cells and mesenchymal stem cells promotes macrophage recruitment. *Proceedings of the National Academy of Sciences* **111**, E2120–E2129 (2014).
50. Mak, P. *et al.* ERbeta impedes prostate cancer EMT by destabilizing HIF-1alpha and inhibiting VEGF-mediated snail nuclear localization: implications for Gleason grading. *Cancer Cell* **17**, 319–332 (2010).
51. Dang, C. V. MYC on the Path to Cancer. *Cell* **149**, 22–35 (2012).
52. Vogt, P. K. Jun, the oncoprotein. *Oncogene* **20**, 2365–2377 (2001).
53. Weili, Z., Zhikun, L., Jianmin, W. & Qingbao, T. Knockdown of USP28 enhances the radiosensitivity of esophageal cancer cells via the c-Myc/hypoxia-inducible factor-1 alpha pathway. *Journal of Cellular Biochemistry* **120**, 201–212 (2019).
54. Liang, S.-H. *et al.* The hyphal-specific toxin candidalysin promotes fungal gut commensalism. *Nature* **627**, 620–627 (2024).
55. Nikou, S.-A. *et al.* The Candida albicans toxin candidalysin mediates distinct epithelial inflammatory responses through p38 and EGFR-ERK pathways. *Science Signaling* **15**, eabj6915 (2022).
56. Richardson, J. P. *et al.* Candidalysins Are a New Family of Cytolytic Fungal Peptide Toxins. *mBio* **13**, e0351021 (2022).
57. Zhang, Z. *et al.* Gut fungi enhances immunosuppressive function of myeloid-derived suppressor cells by activating PKM2-dependent glycolysis to promote colorectal tumorigenesis. *Experimental Hematology & Oncology* **11**, 88 (2022).
58. Narunsky-Haziza, L. *et al.* Pan-cancer analyses reveal cancer-type-specific fungal ecologies and bacteriome interactions. *Cell* **185**, 3789-3806.e17 (2022).
59. Wu, Y. *et al.* Ultrasound Control of Genomic Regulatory Toolboxes for Cancer Immunotherapy. *Nat Commun* **15**, 10444 (2024).

60. Sun, K. Ktrim: an extra-fast and accurate adapter- and quality-trimmer for sequencing data. *Bioinformatics* **36**, 3561–3562 (2020).
61. Dobin, A. *et al.* STAR: ultrafast universal RNA-seq aligner. *Bioinformatics* **29**, 15–21 (2013).
62. Liao, Y., Smyth, G. K. & Shi, W. featureCounts: an efficient general purpose program for assigning sequence reads to genomic features. *Bioinformatics* **30**, 923–930 (2014).
63. Love, M. I., Huber, W. & Anders, S. Moderated estimation of fold change and dispersion for RNA-seq data with DESeq2. *Genome Biology* **15**, 550 (2014).
64. Yu, G., Wang, L.-G., Han, Y. & He, Q.-Y. clusterProfiler: an R Package for Comparing Biological Themes Among Gene Clusters. *OMICS* **16**, 284–287 (2012).
65. Subramanian, A. *et al.* Gene set enrichment analysis: A knowledge-based approach for interpreting genome-wide expression profiles. *Proceedings of the National Academy of Sciences* **102**, 15545–15550 (2005).
66. Sato, T. *et al.* Long-term expansion of epithelial organoids from human colon, adenoma, adenocarcinoma, and Barrett's epithelium. *Gastroenterology* **141**, 1762–1772 (2011).
67. He, G.-W. *et al.* Optimized human intestinal organoid model reveals interleukin-22-dependency of paneth cell formation. *Cell Stem Cell* **29**, 1333-1345.e6 (2022).